



# A multiparametric approach to predict triple-negative breast cancer including parameters derived from ultrafast dynamic contrast-enhanced MRI

Akane Ohashi<sup>1,2,3</sup> · Masako Kataoka<sup>3</sup> · Mami Iima<sup>3,4</sup> · Maya Honda<sup>3,5</sup> · Rie Ota<sup>6</sup> · Yuta Urushibata<sup>7</sup> · Marcel Dominik Nickel<sup>8</sup> · Masakazu Toi<sup>9</sup> · Sophia Zackrisson<sup>1,2</sup> · Yuji Nakamoto<sup>3</sup>

Received: 3 July 2022 / Revised: 12 March 2023 / Accepted: 21 March 2023 / Published online: 8 June 2023

© The Author(s), under exclusive licence to European Society of Radiology 2023

## Abstract

**Objective** Triple-negative breast cancer (TNBC) is a highly proliferative breast cancer subtype. We aimed to identify TNBC among invasive cancers presenting as masses using maximum slope (MS) and time to enhancement (TTE) measured on ultrafast (UF) DCE-MRI, ADC measured on DWI, and rim enhancement on UF DCE-MRI and early-phase DCE-MRI.

**Methods** This retrospective single-center study, between December 2015 and May 2020, included patients with breast cancer presenting as masses. Early-phase DCE-MRI was performed immediately after UF DCE-MRI. Interrater agreements were evaluated using the intraclass correlation coefficient (ICC) and Cohen's kappa. Univariate and multivariate logistic regression analyses of the MRI parameters, lesion size, and patient age were performed to predict TNBC and create a prediction model. The programmed death-ligand 1 (PD-L1) expression statuses of the patients with TNBCs were also evaluated.

**Results** In total, 187 women (mean age, 58 years ± 12.9 [standard deviation]) with 191 lesions (33 TNBCs) were evaluated. The ICC for MS, TTE, ADC, and lesion size were 0.95, 0.97, 0.83, and 0.99, respectively. The kappa values of rim enhancements on UF and early-phase DCE-MRI were 0.88 and 0.84, respectively. MS on UF DCE-MRI and rim enhancement on early-phase DCE-MRI remained significant parameters after multivariate analyses. The prediction model created using these significant parameters yielded an area under the curve of 0.74 (95% CI, 0.65, 0.84). The PD-L1-expressing TNBCs tended to have higher rim enhancement rates than the non-PD-L1-expressing TNBCs.

**Conclusion** A multiparametric model using UF and early-phase DCE-MRI parameters may be a potential imaging biomarker to identify TNBCs.

**Clinical relevance statement** Prediction of TNBC or non-TNBC at an early point of diagnosis is crucial for appropriate management. This study offers the potential of UF and early-phase DCE-MRI to offer a solution to this clinical issue.

## Key Points

- It is crucial to predict TNBC at an early clinical period.
- Parameters on UF DCE-MRI and early-phase conventional DCE-MRI help in predicting TNBC.
- Prediction of TNBC by MRI may be useful in determining appropriate clinical management.

**Keywords** Breast · Breast neoplasms · Magnetic resonance imaging · Triple-negative breast neoplasms · Biomarkers

✉ Masako Kataoka  
makok@kuhp.kyoto-u.ac.jp

<sup>1</sup> Department of Translational Medicine, Diagnostic Radiology, Lund University, Malmö, Sweden

<sup>2</sup> Department of Imaging and Functional Medicine, Skåne University Hospital, Malmö, Sweden

<sup>3</sup> Department of Diagnostic Imaging and Nuclear Medicine, Kyoto University Graduate School of Medicine, 54 Kawahara-Cho Shogoin Sakyo-Ku, Kyoto-Shi, Kyoto, Japan

<sup>4</sup> Institute of Advancement of Clinical and Translational Science (iACT), Kyoto University Hospital, Kyoto, Japan

<sup>5</sup> Department of Diagnostic Radiology, Kansai Electric Power Hospital, Osaka, Japan

<sup>6</sup> Department of Radiology, Tenri Hospital, Nara, Japan

<sup>7</sup> Siemens Healthcare K.K, Shinagawa, Tokyo, Japan

<sup>8</sup> Siemens Healthcare GmbH, Erlangen, Germany

<sup>9</sup> Department of Breast Surgery, Kyoto University Graduate School of Medicine, Kyoto, Japan

## Abbreviations

ADC	Apparent diffusion coefficient
DWI	Diffusion-weighted imaging
ER	Estrogen receptor
HER2	Human epidermal growth factor receptor 2
MS	Maximum slope
PR	Progesterone receptor
TNBC	Triple-negative breast cancer
TTE	Time to enhancement
UF DCE-MRI	Ultrafast dynamic contrast-enhanced magnetic resonance imaging

## Introduction

Breast dynamic contrast-enhanced magnetic resonance imaging (DCE-MRI) has been the most sensitive modality in differentiating benign from malignant breast lesions during the past two decades. Its use has been expanded to preoperative evaluation and early prediction of chemotherapy response [1]. Recently, MRI-based biomarkers have been of interest in predicting breast cancer subtypes [2–4]. One prognostic factor of breast cancer is the intrinsic molecular subtype [5, 6]. Triple-negative breast cancer (TNBC) is a breast cancer subtype defined as lacking the expressions of estrogen receptor (ER), progesterone receptor (PR), and human epidermal receptor 2 (HER-2). It has a poor prognosis because of its aggressive growth, high proliferation, and frequent metastasis. TNBC responds to chemotherapy in spite of having a prognosis worse than those of other breast cancer subtypes [7, 8]. Therefore, it is crucial to predict whether breast cancer is TNBC or non-TNBC as early as possible in the diagnostic process and use MRI findings to plan the preoperative treatment, which may also affect long-term prognosis [9]. In addition, 20% of TNBCs have elevated programmed death-ligand 1 (PD-L1) expression levels, a higher rate than that in non-TNBCs ( $p < 0.001$ ) [10]. Immunotherapy targeting PD-L1 could improve the clinical outcomes of early-stage PD-L1-expressing TNBC [11]. Therefore, when selecting patients for immunotherapy, differentiating PD-L1-expressing TNBCs based on MRI findings could provide meaningful information.

Several studies have evaluated TNBCs using various MRI parameters. These studies have suggested that the following are important parameters for predicting TNBCs: high perfusion on conventional DCE-MRI [12], a relatively high apparent diffusion coefficient (ADC) value on diffusion-weighted imaging (DWI) [13–15], and rim enhancement based on morphological information [2, 3, 13].

Ultrafast (UF) DCE-MRI enables the evaluation of tumor vascularity in a much shorter scanning time than

conventional DCE-MRI. The diagnostic performance of UF parameters (maximum slope (MS), time to enhancement (TTE), and bolus arrival time) in differentiating benign from malignant breast lesions has been reported to be higher than or equal to that of conventional DCE-MRI parameters [16–18]. Furthermore, some evidence exists that supports the usefulness of UF DCE-MRI parameters for the identification of breast cancer subtypes or prognostic factors [19–21].

The ADC, calculated using the signal intensity changes on DWI with two or more  $b$  values, is useful in the diagnosis of malignant breast cancer [22]. Previous studies have investigated the relationship between the molecular subtypes of breast cancer and ADC values measured on DWI [13, 23, 24]. Youk et al. [13] suggested that the mean ADC value of TNBCs was higher than that of ER-positive and HER2-positive breast cancers ( $p < 0.0001$ ). The higher ADC value in TNBC than in other subtypes may reflect intratumoral necrosis [2].

Uematsu et al. [2] and Youk et al. [13] suggested that the presence of a mass lesion and rim enhancement were significantly associated with TNBC. However, they evaluated rim enhancement on conventional DCE-MRI alone. In our experience, the frequency of rim enhancement may differ between UF and conventional DCE-MRI because of the heterogeneity of the enhancement patterns in a lesion.

Several studies have used MRI parameters to predict TNBC, but studies that used UF DCE-MRI have been limited. Moreover, no reported evidence has shown the usefulness of UF DCE-MRI parameters in predicting PD-L1-expressing TNBCs.

The purpose of this study was to identify the clinically adaptable imaging biomarkers to predict TNBC using a multiparametric model based on the significant parameters identified from the following MRI parameters: MS and TTE on UF DCE-MRI, ADC on DWI, and rim enhancement on UF DCE-MRI and early-phase DCE-MRI. In addition, we aimed to predict PD-L1-expressing TNBC cases using MRI parameters.

## Materials and methods

### Study population

The study protocol was approved by our institutional review board. Owing to the retrospective study design, the requirement for informed consent was waived. The study population included consecutive patients who underwent breast MRI, including UF DCE-MRI combined with conventional DCE-MRI, between December 2015 and May 2020. Data on patients were obtained using a database from the picture archiving and communication system and clinical

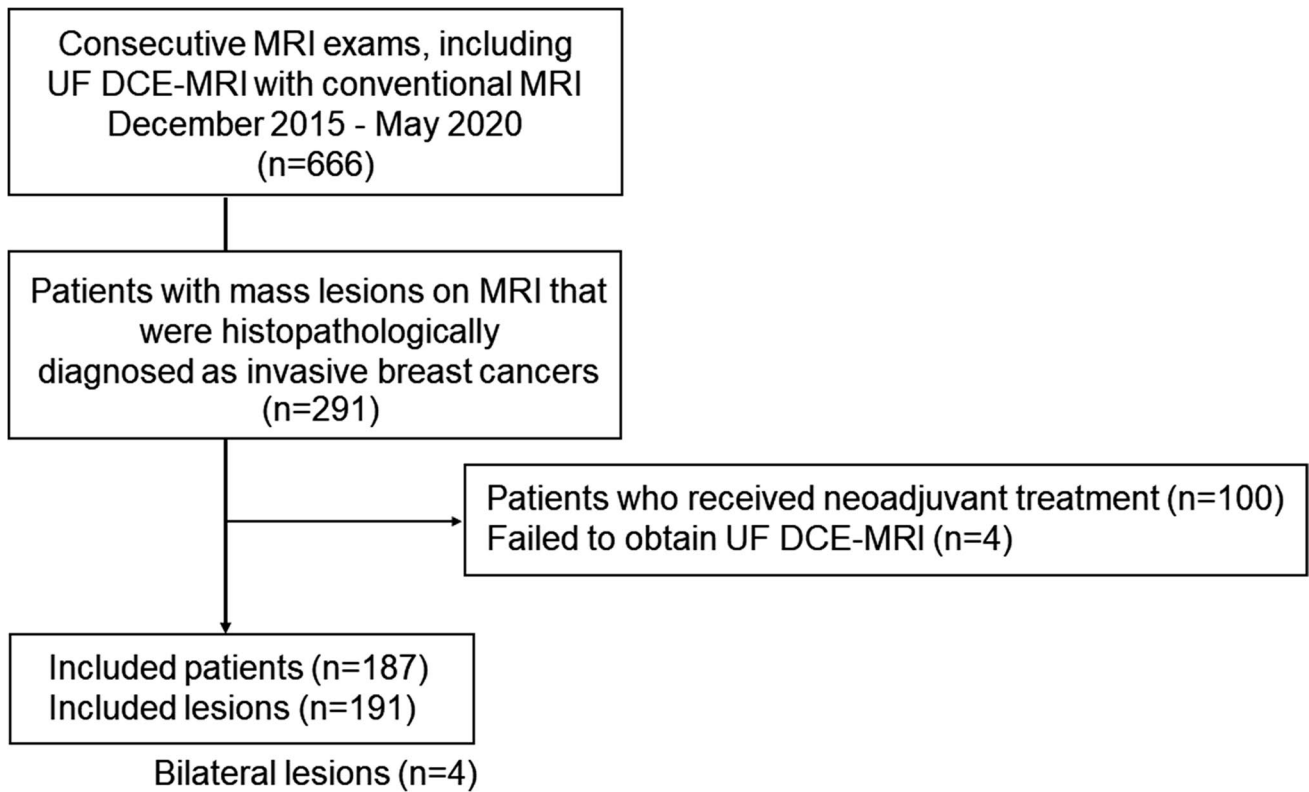


**Fig. 1** Flowchart of the study population. *UF* ultrafast

records of our hospital. UF DCE-MRI was performed for patients with known lesions detected with other imaging modalities (mammography and ultrasonography), patients aged  $\leq 50$  years, and patients who showed marked background parenchymal enhancement on a previous MRI scan.

In total, 291 patients with mass lesions on MRI (morphological information from the Breast Imaging Reporting and Data System [25]) that were histopathologically diagnosed as invasive breast cancers were identified. One hundred patients were excluded because they had received neoadjuvant chemotherapy or

neoadjuvant endocrine therapy. Four patients were also excluded because of failed image acquisition. In cases with multiple mass lesions in the breast, the largest lesion was selected. Finally, 187 patients with a total of 191 lesions were included, of whom four had bilateral lesions (Fig. 1). An analysis was performed per lesion. Parts of the study population in this study had been included in the two papers previously. The first study used kinetic parameters measured on UF DCE-MRI to distinguish benign and malignant lesions [26]. The second study compared morphological information between UF and

**Table 1** Pathological diagnosis and subtype classifications of mass-forming breast cancers ( $n = 191$ )

	Total	Luminal A	Luminal B	HER-2	TNBC
NST	162	58	72	9	23
ILC	8	4	4	0	0
Mucinous carcinoma	7	4	2	1	0
Invasive micropapillary carcinoma	3	2	0	0	1
Invasive carcinoma with apocrine differentiation *	6	0	0	0	6
Histiocytoid carcinoma	2	0	0	0	2
Other	3	2	0	0	1
Total	191	70	78	10	33

*NST*, no special type; *ILC*, invasive lobular carcinoma; *LA*, luminal A-like; *LB*, luminal B-like; *HER2*, epidermal growth factor receptor type 2-enriched; *TNBC*, triple-negative breast cancer

\*Including one lesion with metaplastic component

conventional DCE MR images [27]. In contrast, the present study used kinetic parameters measured on UF DCE-MRI to identify TNBCs among known mass-forming cancers. Table 1 shows the detailed pathological diagnoses of the lesions included in this study. The World Health Organization classification of breast cancer was used to classify the pathological diagnoses [28]. The histopathological evaluation is detailed in Appendix 1.

### MRI acquisition protocols

Breast MRI was performed in the prone position using a 3-T scanner (MAGNETOM Skyra or Prisma, Siemens Healthcare GmbH) with a dedicated 16- or 18-channel bilateral breast coil. The detailed scan protocols for conventional DCE-MRI, UF DCE-MRI, and DWI sequences are shown in Table 2.

After the pre-contrast phase of conventional DCE-MRI, a UF DCE-MRI scan was acquired as follows: 15 s before contrast injection to 60 s after contrast injection and 2-s preparation time followed by 20 continuous phases taken at a rate of 3.7 s/phase. The early-phase (1–2 min after contrast injection) and delayed-phase conventional DCE-MRI (5–6 min) were acquired. The contrast agent, gadobutrol (Gadovist, Bayer AG), was infused intravenously at a dose of 0.1 mL/kg and a speed of 2.0 mL/s. A 20-mL saline bolus was then administered at the same rate. UF DCE-MRI was performed using a prototypical three-dimensional gradient-echo volumetric interpolated breath-hold examination sequence with compressed sensing reconstruction (30 iterations using a separate retrospective evaluation of the convergence speed). See [26] for more details.

### Image analysis

The inflow of contrast agents on UF DCE-MRI was analyzed using dedicated prototype software (MR DCE ver. 1.1.0, Siemens Healthcare GmbH). The analysis included two kinetic parameters measured on UF DCE-MRI: MS and TTE. A schematic explanation of the UF DCE-MRI parameters is shown in Fig. 2.

MS was calculated as the change in relative enhancement among three time points, divided by the time, and summarized as the percentage of relative enhancement per second (%/s). TTE was calculated as the time interval between the start of enhancement at the aorta and that at the lesion. Three-millimeter circular regions of interest (ROI) were manually marked on the lesion in color-coded MS and TTE maps to quantify the value of the highest MS and shortest TTE, and their mean values were recorded.

ADC maps derived from DWI were generated with a logarithmic equation (see Appendix 2). Three-millimeter circular ROI was manually marked on the restricted diffusion area inside the lesion on the ADC maps to quantify the lowest ADC value with reference to DCE-MRI and DWI, and the mean value was recorded.

The ROI was selected separately for each acquisition, avoiding cystic, necrotic, fatty, and hemorrhagic areas. A representative TNBC case with four different quantitative images is shown in Fig. 3.

Rim enhancement from morphological information was visually evaluated. The presence or absence of rim enhancement was recorded from the 20th (final) phase of UF DCE-MRI and the early phase of conventional DCE-MRI. In addition, the tumor size was measured in the largest section

**Table 2** Scan protocol of conventional DCE MRI, UF DCE-MRI, and DWI

	Conventional DCE MRI	UF DCE-MRI	DWI
Sequence	VIBE with FS	VIBE without FS	Axial, SS-EPI, 3D FLASH
TR/TE (ms)	3.8/ 1.4	5.0/ 2.5 <sup>*1</sup> , 4.8/ 2.5 <sup>*2</sup>	9200/ 57 <sup>*1</sup> , 5600–6300/ 48–50 <sup>*2</sup>
Flip angle (degree)	15	15	90
Slice thickness (mm)	1.0	2.5	3.0
FOV (mm)	330×330	360×360	330×185.4
Resolution (mm)	0.86×0.86 (144 slices)	0.94×0.94 (60 slices)	2.0×2.0 (48 slices)
Matrix <sup>*3</sup>	384×384	384×384	162×92
Fat-suppression	SPAIR	None	SPAIR
Number of time points (s/frame)	60 [pre, early, delay]	3.7 [20 frames]	
<i>b</i> -value (sec/mm <sup>2</sup> )			0, 1000

VIBE, volumetric interpolated breath-hold examination; FS, fat suppression; TR/TE, repetition time/echo time; FOV, field of view; SPAIR, spectral attenuated inversion recovery

<sup>\*1</sup> MAGNETOM Skyra

<sup>\*2</sup> MAGNETOM Prisma

<sup>\*3</sup> Reconstructed matrix

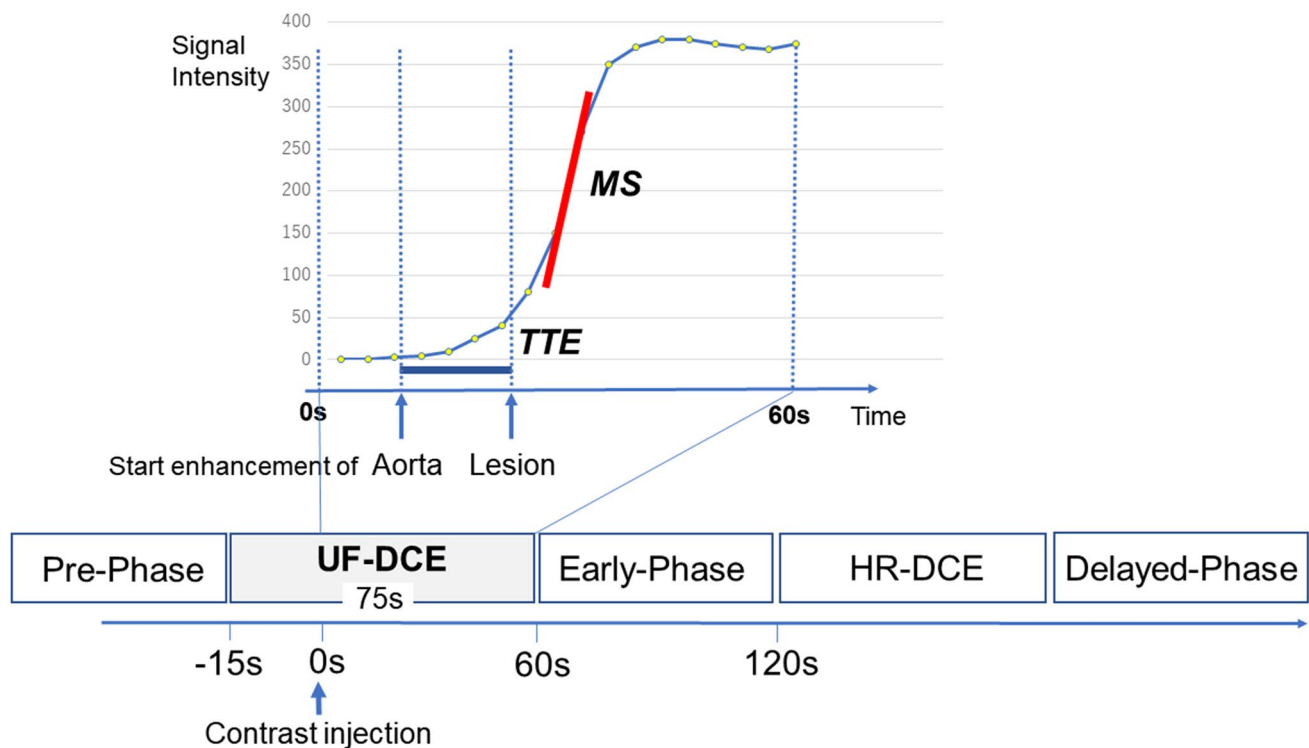


**Fig. 2** Schematic explanation of the UF DCE-MRI parameters. Our dynamic protocols, including UF DCE-MRI, are shown. UF DCE-MRI using improved VIBE: 20 frames (pre + 19 frames), 3.7 s/frame. MS is the slope of the tangent (%/s) along the steepest part of the curve. TTE is the time interval between the start of enhancement of

the aorta and that of the lesion. *UF* ultrafast, *VIBE* volumetric interpolated breath-hold examination, *MS* maximum slope, *TTE* time to enhancement, *HR-DCE-MRI* high-resolution dynamic contrast-enhanced magnetic resonance imaging

of the lesion on the axial image at the early phase of conventional DCE-MRI.

Two independent radiologists specializing in breast imaging recorded the quantitative values of MS, TTE, ADC, lesion size, and rim enhancement. Three radiologists (radiologist 1, 2, 3 for A.O., M.K., and M.H.) were involved and had 7, 22, and 5 years of experience in diagnosing breast MRI, respectively. The MS, TTE, lesion size, and rim enhancement were measured by radiologists 1 and 2, and the ADC values were measured by radiologists 1 and 3, independently.

### Statistical analyses

The interrater agreements for the quantitative parameters (MS, TTE, ADC, and lesion size) were evaluated using intraclass correlation coefficients (ICCs), and the qualitative parameters (presence of rim enhancement on UF and conventional DCE-MRI) were assessed using Cohen's kappa. ICCs of  $\leq 0.40$  indicated poor agreement; 0.40 to 0.59, fair agreement; 0.60 to 0.74, good agreement; and 0.75 to 1.00, excellent agreement. Kappa values of 0.01 to 0.20 indicated slight agreement; 0.21 to 0.40, fair agreement; 0.41 to 0.60, moderate agreement; 0.61 to 0.80, substantial agreement;

and 0.81 to 1.00, almost perfect agreement. To use reliable values for subsequent analyses, for quantitative parameters with an ICC greater than 0.75 (excellent agreement), the values of the two readers were averaged. For qualitative parameters with kappa values greater than 0.81 (nearly perfect agreement), discrepant cases were reconfirmed through a consensus between the two readers. The final decision was used for subsequent analysis.

The Mann–Whitney *U* test was used to compare all quantitative parameters (MS, TTE, ADC, lesion size, and patient age) and the frequency of rim enhancement between TNBC and non-TNBC. For the sub-analysis, the same test was used to compare all quantitative parameters between the PD-L1- and non-PD-L1-expressing TNBCs.

A univariate logistic regression analysis was performed to select the significantly contributing parameters ( $p < 0.05$ ) to the prediction of TNBC. The selected independent significant parameters ( $p < 0.05$ ) were used in the multivariate logistic regression analysis and multiparametric prediction model to predict the probability of TNBC. When two parameters from the same categories were significant, the one with the smallest *p* value was selected as the representative parameter. Such parameter pairs included UF DCE-MRI-derived parameters (MS or TTE) and the presence of rim



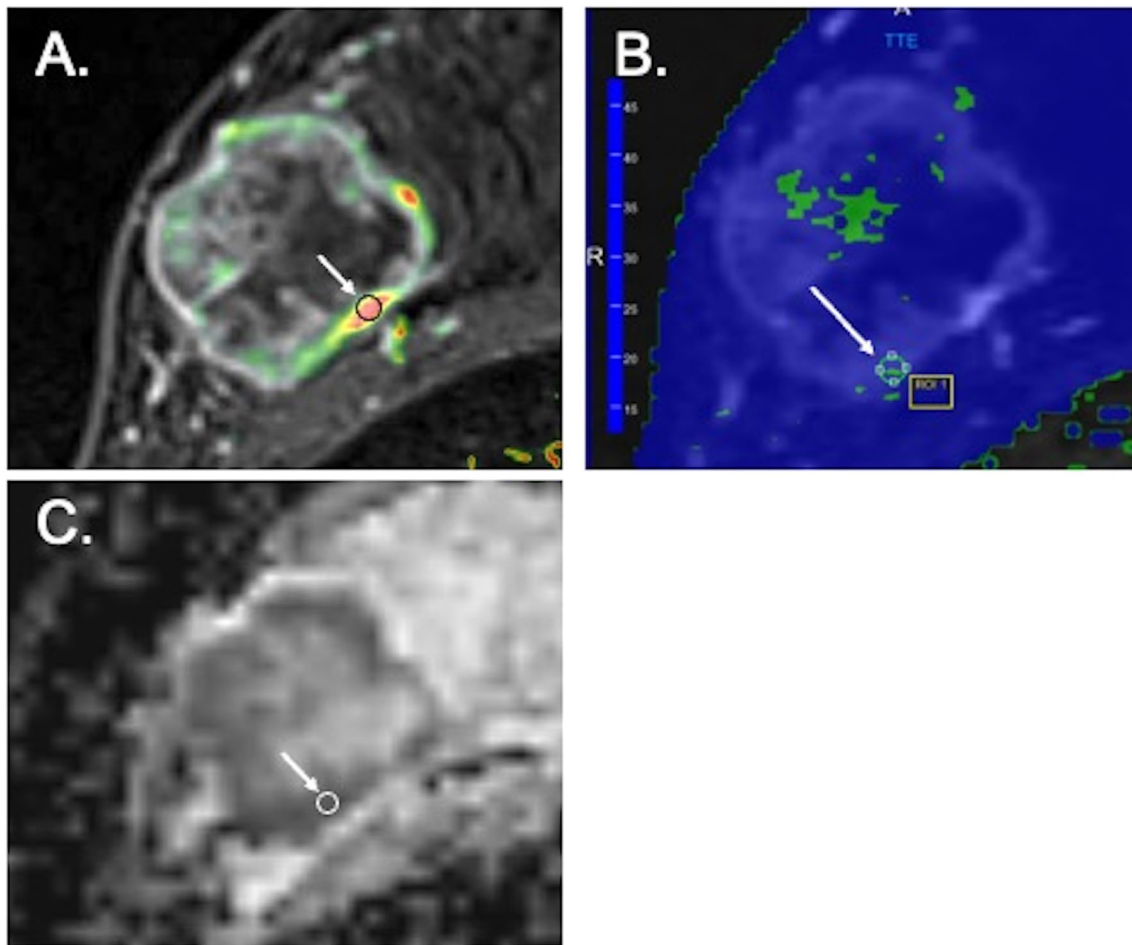


**Fig. 3** Representative case of TNBC with three different quantitative maps. **A** Color-coded MS map. The highest MS was selected using a 3-mm circular ROI. **B** Color-coded TTE map. The lowest TTE was selected using a 3-mm circular ROI. **C** ADC map derived from DWI.

The lowest mean ADC was selected using a 3-mm circular ROI. *TNBC* triple-negative breast cancer, *MS* maximum slope, *TTE* time to enhancement, *ROI* region of interest

enhancement (on UF DCE-MRI or conventional DCE-MRI). The area under the receiver-operating characteristic (ROC) curve was used to evaluate the diagnostic performance of the model. The Youden index, based on the maximum value of the sum of the sensitivity and specificity, was used to determine the optimal cutoff value of the prediction model.

For the statistical analyses, EZR (Saitama Medical Center, Jichi Medical University) [29] and MedCalc version 20.008 (MedCalc Software) were used. All  $p$  values were two-sided, and  $p$  values  $<0.05$  were considered statistically significant.

## Results

One hundred ninety-one mass lesions from 187 patients (age range, 31–87 years; mean, 58 years) were examined, including 33 TNBCs and 158 non-TNBCs.

## MRI parameters

The interrater agreements for MS, TTE, ADC, and lesion size were excellent (ICCs: 0.95, 0.97, 0.83, and 0.99, respectively). Therefore, for these parameters, the measurement results from the two radiologists were averaged for the analysis. The interrater agreement for rim enhancement on UF and conventional DCE-MRI was close to perfect (kappa values: 0.88 and 0.84, respectively). Therefore, the discrepancy values were reevaluated by a consensus assessment for analysis.

The averaged mean  $\pm$  standard deviation of all quantitative parameters and the number and percentage of rim enhancement between the TNBCs and non-TNBCs are shown in Table 3. The MS was higher, TTE was lower, and lesion size was larger in the TNBCs than in the non-TNBC (MS: 30.0%/s vs. 24.1%/s,  $p=0.005$ ; TTE: 4.3 vs. 5.9 s,  $p=0.02$ ; and size: 24.0 vs. 18.5 mm,  $p=0.002$ , respectively). Age and ADC value did not show significant differences between TNBC

**Table 3** Comparison of the quantitative and qualitative parameters between the TNBCs ( $n=33$ ) and non-TNBCs ( $n=158$ )

	TNBC	Non-TNBC	$p$ value
Quantitative parameters			
Age (y)	60.0 [13.3]	58.0 [12.9]	0.68
Size (mm)	24.0 [19.9]	18.5 [15.2]	0.002*
UF DCE-MRI			
MS (%/s)	30.0 [10.7]	24.1 [10.9]	0.005*
TTE (s)	4.3 [2.6]	5.9 [3.0]	0.02*
DWI			
ADC ( $\times 10^{-3}\text{mm}^2/\text{s}$ )	0.8 [0.1]	0.8 [0.2]	0.32
Qualitative parameters			
Presence of rim enhancement no. /total no. (%)			
On UF DCE-MRI	22/ 33 (66.7)	59/ 158 (37.3)	0.002*
On early-phase DCE-MRI	27/ 33 (81.8)	77/158 (48.7)	<0.001*

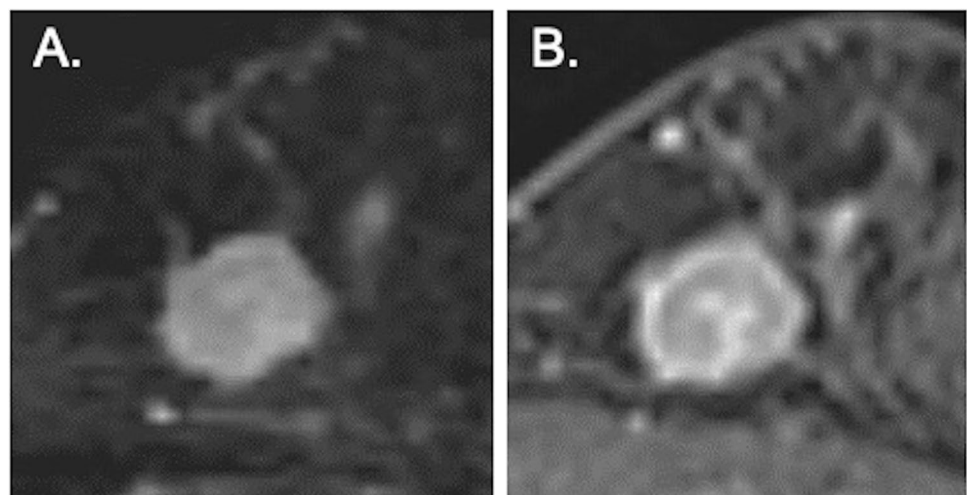
The values of quantitative parameters are means and those in brackets are standard deviations. The values of the parameters and number of parameters were compared between the TNBCs and non-TNBCs using the Mann–Whitney  $U$  test

*UF-DCE MRI* ultrafast dynamic contrast MRI, *TNBC* triple-negative breast cancer, *MS* maximum slope, *TTE* time to enhancement, *ADC* apparent diffusion coefficient

\*Factors that remained statistically significant ( $p < 0.05$ )

and non-TNBC ( $p = 0.68, 0.32$  respectively). The percentage of rim enhancement on both UF and conventional DCE-MRI was higher among the TNBCs than the non-TNBCs. It was higher on conventional DCE-MRI than on UF DCE-MRI (TNBC vs. non-TNBC: UF DCE-MRI: 66.7% vs. 37.0%,  $p = 0.002$ ; conventional DCE-MRI: 81.8% vs. 48.7%,  $p < 0.001$ ). A representative TNBC case is shown in Fig. 4. Rim enhancement was more clearly visible on conventional DCE-MRI than on the last phase of UF DCE-MRI.

**Fig. 4** A representative case of TNBC presenting as a mass lesion. The rim enhancement is more clearly visible on conventional DCE-MRI than on the last-phase UF DCE-MRI. **A** The final phase (20th) of UF DCE-MRI (no rim enhancement). **B** The early phase of conventional DCE-MRI (with rim enhancement). *TNBC* triple-negative breast cancer, *UF* ultrafast



## Diagnostic performance

The univariate logistic regression analysis revealed that the MS and TTE on UF DCE-MRI, and lesion size and rim enhancement on UF and conventional DCE-MRI were independently associated with TNBC (Table 4). The MS on UF DCE-MRI, and lesion size and rim enhancement on conventional DCE-MRI were selected for the multivariate logistic regression analysis. The analysis revealed that the MS on UF DCE-MRI and rim enhancement on conventional DCE-MRI were independently associated with TNBC ( $p = 0.03$  and  $p = 0.002$ , respectively; Table 4). The ROC curve of the multiparametric prediction model combining MS and rim enhancement on conventional DCE-MRI demonstrated an area under the ROC curve (95% confidence interval) of 0.74 (0.65–0.84) (Fig. 5). Using the optimal cutoff value for the prediction model resulted in a sensitivity and specificity of 72.7% and 68.4%, respectively.

## Sub-analysis

Among nine TNBCs (from September 2019), seven lesions expressed PD-L1, whereas two lesions did not. The MS was lower in the PD-L1-expressing lesions than in the PD-L1-negative lesions, with mean values of 25.7%/s and 48.0%/s, respectively. Among the seven PD-L1-expressing lesions, six lesions showed rim enhancement on conventional DCE-MRI (85.7%) and five lesions showed rim enhancement on UF DCE-MRI (71.4%). The values of all parameters for the PD-L1 expressing TNBCs are shown in Appendix Table 1.

**Table 4** Univariate and multivariate logistic regression analyses for the prediction of TNBC and non-TNBC

Parameters	Univariate logistic regression analysis	<i>p</i> value	Multivariate logistic regression analysis	<i>p</i> value
Age (y)	1.01 [0.98–1.04]	0.692		
Size (mm)	1.03 [1.01–1.05]	0.012 *	1.01 [0.99–1.03]	0.290
UF DCE-MRI				
MS (%/s)	1.05 [1.05–1.08]	0.008 *	1.04 [1.00–1.08]	0.033*
TTE (s)	0.86 [0.75–0.98]	0.025 *		
DWI				
ADC ( $\times 10^{-3}$ mm <sup>2</sup> /s)	0.79 [0.10–6.18]	0.824		
Rim enhancement				
On UF DCE-MRI	3.36 [1.52–7.4]	0.003 *		
On early phase of DCE-MRI	4.73 [1.85–12.1]	0.001 *	4.47 [1.71–11.7]	0.002*

Data are presented as odds ratio and data in brackets are 95% confidence interval

UF-DCE MRI ultrafast dynamic contrast MRI, TNBC triple-negative breast cancer, MS maximum slope, TTE time to enhancement, ADC apparent diffusion coefficient

\*Factors that remained statistically significant ( $p < 0.05$ )

## Discussion

This study suggests that the combination of MS on UF DCE-MRI and rim enhancement on early-phase conventional DCE-MRI can be used to identify TNBCs among invasive breast cancers presenting as masses. UF DCE-MRI parameters may reflect the high perfusion state of TNBC. A

high MS indicates fast contrast inflow into the lesion, and a shorter TTE indicates early contrast inflow into the lesion.

Although this is a new technique and the number of available facilities is limited, UF DCE-MRI can solve the problems of high cost and time required in the use of conventional MRI by enabling high spatial and temporal resolutions. No previous reports have used this technique as an imaging biomarker to differentiate TNBC itself. The results of a previous study that used conventional DCE-MRI parameters suggested that lower extracellular space (higher cell density) and higher contrast agent washout rate (higher vascular permeability) are significant predictors of TNBC [12]. Other studies have demonstrated that a shorter bolus arrival time and shorter TTE measured on UF DCE-MRI are significant predictors of aggressive breast cancer subtypes such as TNBC or HER-2 [19, 20]. Our results regarding the TTE in TNBC are consistent with their results. MS reflects the perfusion information of breast lesions, as did TTE or bolus arrival time, and may have the potential to identify TNBC, as demonstrated in our study. Further research on perfusion parameters using UF DCE-MRI in breast cancer subtypes is needed.

In our study, the UF DCE-MRI parameters were more predictive of TNBC than ADC. Previous studies have also shown that higher ADC values were significantly associated with TNBC using the whole-lesion ROI (the area with the entire tumor) [13, 15, 23]. However, our study results showed no significant difference in ADC value between the TNBCs and non-TNBCs ( $p = 0.32$ ; Table 3). This discrepancy may be due to the measurement technique for ADC. The ADC value was measured as the area with the most restricted diffusion in the lesion on the ADC maps to quantify the lowest ADC value in our study. This ADC

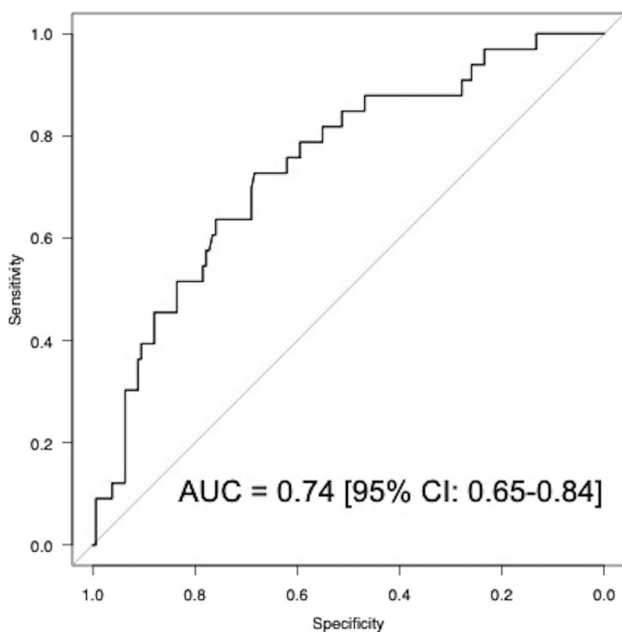


**Fig. 5** ROC curve of a multiparametric prediction model for TNBC that combines MS and presence of rim enhancement in the early phase of conventional DCE-MRI. The area under the ROC curve is 0.74 (95% confidence interval, 0.65–0.84). TNBC triple-negative breast cancer, MS maximum slope



measurement method can effectively predict malignant lesions [26], but not TNBCs.

Our results showed that rim enhancement was highly associated with TNBC, as in previous studies [2, 3, 13, 15, 30, 31]. However, our research differs from previous studies in that it evaluated rim enhancement based on images acquired at two different time points: the last phase of UF DCE-MRI and the early phase of conventional DCE-MRI. The rim enhancement at both time points showed a strong association with TNBC ( $p < 0.05$ ). However, the percentage of rim enhancement on conventional DCE-MRI was much higher than that on UF DCE-MRI (81.8% vs. 48.7%), which suggests that the early phase of conventional DCE-MRI may be better suited for morphology-based subtype estimation. Although a previous study indicated that the presence of rim enhancement is related to prognosis [3], the optimal timing that can accurately determine the presence of rim enhancement should be considered. In addition, a previous study showed that compared with delayed rim enhancement, early rim enhancement correlated with the microvessel densities in the peripheral areas of breast mass lesions and vascular endothelial growth factor expression [32]. Further research is needed to confirm the pathological features associated with UF DCE-MRI.

Our report is the first study to evaluate the PD-L1 expression levels of TNBCs using UF DCE-MRI. PD-L1-expressing TNBC lesions tended to have a high rate of rim enhancement and lower MS than the non-PD-L1-expressing lesions. The small number of cases in the present study is insufficient to show a tendency; thus, further studies are needed. In selecting patients for immunotherapy, it would be meaningful to differentiate the PD-L1 expression in TNBCs using MRI information.

Although this study alone is insufficient to recommend that biopsy can be avoided in identifying TNBC, predicting the likelihood of TNBC at the time of preoperative MRI may be helpful in determining preoperative chemotherapy. The measurements in this study were performed manually by the readers. If artificial intelligence can automatically place ROI and determine the presence of rim enhancement on images, this could help radiologists make a rapid diagnosis and reduce the reading time.

The limitations of this study include its retrospective design and relatively small sample size, especially in cases evaluated for the presence of PD-L1 expression. In addition, the study population excluded patients with noninvasive carcinoma and benign lesions, which differs from the normal lesion distribution in clinical settings. Finally, the visual assessment might have been affected by the differences in spatial resolution and image reconstruction methods between UF DCE-MRI and conventional DCE-MRI.

In conclusion, a multiparametric model using MS measured on UF DCE-MRI and rim enhancement in the early phase of conventional DCE-MRI may be a potential imaging biomarker to diagnose TNBC.

**Supplementary Information** The online version contains supplementary material available at <https://doi.org/10.1007/s00330-023-09730-w>.

**Acknowledgements** We thank Dr. Sakurai Takaki and Dr. Tatsuki R. Kataoka for support with the pathological diagnosis. The pathological information was obtained at the Department of Diagnostic Pathology, Graduate School of Medicine, Kyoto University. We thank Libby Cone, MD, MA, from Edanz Group Japan ([www.edanzediting.com/ac](http://www.edanzediting.com/ac)) for editing a draft of this manuscript.

**Funding** This work was supported by a Tumor vascularity and tumor-related vessels using ultrafast DCE MRI of the Breast Grants-in-Aid for Scientific Research Grant-in-Aid for Scientific Research (C), Japan Society for the Promotion of Science, Apr, 2018–Mar, 2021 (18K07673).

## Declarations

**Guarantor** The scientific guarantor of this publication is Akane Ohashi, MD, PhD.

**Conflict of interest** Marcel Dominik Nickel, PhD, is employed by Siemens Healthcare GmbH, Germany, and Yuta Urushibata is employed by Siemens Healthcare K.K.

The remaining authors of this manuscript declare no relationships with any companies, whose products or services may be related to the subject matter of the article.

**Statistics and biometry** One of the authors has significant statistical expertise.

**Informed consent** Written informed consent was waived by the Institutional Review Board.

**Ethical approval** Institutional Review Board (Kyoto University Graduate School and Faculty of Medicine, Ethics Committee) approval was obtained.

**Study subjects or cohorts overlap** Some study subjects or cohorts have been previously reported in Akane Ohashi, Magnetic Resonance Imaging, 71 (2020) 154–160, “A multiparametric approach to diagnosing breast lesions using diffusion-weighted imaging and ultrafast dynamic contrast-enhanced MRI”.

## Methodology

- retrospective
- diagnostic study
- performed at one institution

## References

1. Mann RM, Hooley R, Barr RG, Moy L (2020) Novel approaches to screening for breast cancer. *Radiology* 297:266–285
2. Uematsu T, Kasami M, Yuen S (2009) Triple-negative breast cancer: correlation between MR imaging and pathologic findings. *Radiology* 250:638–647. <https://doi.org/10.1148/radiol.2503081054>
3. Schmitz AMT, Loo CE, Wesseling J et al (2014) Association between rim enhancement of breast cancer on dynamic contrast-enhanced MRI and patient outcome: impact of subtype. *Breast Cancer Res Treat* 148:541–551. <https://doi.org/10.1007/s10549-014-3170-9>

4. Luo HB, Du MY, Liu YY et al (2020) Differentiation between luminal A and B molecular subtypes of breast cancer using pharmacokinetic quantitative parameters with histogram and texture features on preoperative dynamic contrast-enhanced magnetic resonance imaging. *Acad Radiol* 27:e35–e44. <https://doi.org/10.1016/j.acra.2019.05.002>
5. Nguyen PL, Taghian AG, Katz MS et al (2008) Breast cancer subtype approximated by estrogen receptor, progesterone receptor, and HER-2 is associated with local and distant recurrence after breast-conserving therapy. *J Clin Oncol* 26:2373–2378. <https://doi.org/10.1200/JCO.2007.14.4287>
6. Johansson ALV, Trewin CB, Hjerkind KV et al (2019) Breast cancer-specific survival by clinical subtype after 7 years follow-up of young and elderly women in a nationwide cohort. *Int J Cancer* 144:1251–1261. <https://doi.org/10.1002/ijc.31950>
7. Carey L, Winer E, Viale G et al (2010) Triple-negative breast cancer: disease entity or title of convenience? *Nat Rev Clin Oncol* 7:683–692. <https://doi.org/10.1038/nrclinonc.2010.154>
8. Li X, Yang J, Peng L et al (2017) Triple-negative breast cancer has worse overall survival and cause-specific survival than non-triple-negative breast cancer. *Breast Cancer Res Treat* 161:279–287. <https://doi.org/10.1007/s10549-016-4059-6>
9. Ashok Kumar P, Paulraj S, Wang D et al (2021) Associated factors and outcomes of delaying adjuvant chemotherapy in breast cancer by biologic subtypes: a National Cancer Database study. *J Cancer Res Clin Oncol* 147:2447–2458. <https://doi.org/10.1007/s00432-021-03525-6>
10. Mittendorf EA, Philips AV, Meric-Bernstam F et al (2014) PD-L1 expression in triple-negative breast cancer. *Cancer Immunol Res* 2:361–370. <https://doi.org/10.1158/2326-6066.CIR-13-0127>
11. Emens LA, Cruz C, Eder JP et al (2019) Long-term clinical outcomes and biomarker analyses of atezolizumab therapy for patients with metastatic triple-negative breast cancer: a phase I study. *JAMA Oncol* 5:74–82. <https://doi.org/10.1001/jamaoncol.2018.4224>
12. Li SP, Padhani AR, Taylor NJ et al (2011) Vascular characterisation of triple negative breast carcinomas using dynamic MRI. *Eur Radiol* 21:1364–1373. <https://doi.org/10.1007/s00330-011-2061-2>
13. Youk JH, Son EJ, Chung J et al (2012) Triple-negative invasive breast cancer on dynamic contrast-enhanced and diffusion-weighted MR imaging: comparison with other breast cancer subtypes. *Eur Radiol* 22:1724–1734. <https://doi.org/10.1007/s00330-012-2425-2>
14. Kato F, Kudo K, Yamashita H et al (2016) Differences in morphological features and minimum apparent diffusion coefficient values among breast cancer subtypes using 3-tesla MRI. *Eur J Radiol* 85:96–102. <https://doi.org/10.1016/j.ejrad.2015.10.018>
15. İmre Yetkin D, Gulsun Akpınar M, Durhan G, Basaran Demirkazık F (2021) Comparison of clinical and magnetic resonance imaging findings of triple-negative breast cancer with non-triple-negative tumours. *Polish J Radiol* 86:269–276. <https://doi.org/10.5114/pjr.2021.106137>
16. Mann RM, Mus RD, Van Zelst J et al (2014) A novel approach to contrast-enhanced breast magnetic resonance imaging for screening: high-resolution ultrafast dynamic imaging. *Invest Radiol* 49:579–585. <https://doi.org/10.1097/RLL.0000000000000057>
17. Ohashi A, Kataoka M, Kanao S, et al (2019) Diagnostic performance of maximum slope: A kinetic parameter obtained from ultrafast dynamic contrast-enhanced magnetic resonance imaging of the breast using k-space weighted image contrast (KWIC). *Eur J Radiol* 118. <https://doi.org/10.1016/j.ejrad.2019.06.012>
18. Honda M, Kataoka M, Onishi N, et al (2020) New parameters of ultrafast dynamic contrast-enhanced breast MRI using compressed sensing. *J Magn Reson Imaging* 51. <https://doi.org/10.1002/jmri.26838>
19. Onishi N, Sadinski M, Hughes MC et al (2020) Ultrafast dynamic contrast-enhanced breast MRI may generate prognostic imaging markers of breast cancer. *Breast Cancer Res* 22:1–13. <https://doi.org/10.1186/s13058-020-01292-9>
20. Shin SU, Cho N, Kim SY et al (2020) Time-to-enhancement at ultrafast breast DCE-MRI: potential imaging biomarker of tumour aggressiveness. *Eur Radiol* 30:4058–4068. <https://doi.org/10.1007/s00330-020-06693-0>
21. Yamaguchi K, Nakazono T, Egashira R et al (2021) Maximum slope of ultrafast dynamic contrast-enhanced MRI of the breast: comparisons with prognostic factors of breast cancer. *Jpn J Radiol* 39:246–253. <https://doi.org/10.1007/s11604-020-01049-6>
22. Iima M (2020) Diffusion MRI of the breast : current status and future directions. *J Magn Reson Imaging* 52:20–23
23. Liu HL, Zong M, Wei H et al (2019) Added value of histogram analysis of apparent diffusion coefficient maps for differentiating triple-negative breast cancer from other subtypes of breast cancer on standard MRI. *Cancer Manag Res* 11:8239–8247. <https://doi.org/10.2147/CMAR.S210583>
24. Ma Y, Shan D, Wei J, Chen A (2021) Application of intravoxel incoherent motion diffusion-weighted imaging in differential diagnosis and molecular subtype analysis of breast cancer. *Am J Transl Res* 13:3034–3043
25. Morris EA, Comstock CE LC (2013) ACR BI-RADS® Magnetic Resonance Imaging. ACR BI-RADS® Atlas, Breast Imaging Report Data Syst Reston, VA, Am Coll Radiol
26. Ohashi A, Kataoka M, Iima M et al (2020) A multiparametric approach to diagnosing breast lesions using diffusion-weighted imaging and ultrafast dynamic contrast-enhanced MRI. *Magn Reson Imaging* 71:154–160. <https://doi.org/10.1016/j.mri.2020.04.008>
27. Ohashi A, Kataoka M, Iima M et al (2023) Comparison of ultrafast dynamic contrast-enhanced (DCE) MRI with conventional DCE MRI in the morphological assessment of malignant breast lesions. *Diagnostics* 13:1105. <https://doi.org/10.3390/diagnostics13061105>
28. Lakhani SR, Ellis IO, Schnitt SJ, Tan PH van der Vijver M WHO classification of tumors the breast, WHO classification of tumors 4th edition, Volume 4
29. Kanda Y (2013) Investigation of the freely available easy-to-use software “EZR” for medical statistics. *Bone Marrow Transplant* 48:452–458. <https://doi.org/10.1038/bmt.2012.244>
30. Wu M, Ma J (2017) Association between imaging characteristics and different molecular subtypes of breast cancer. *Acad Radiol* 24:426–434. <https://doi.org/10.1016/j.acra.2016.11.012>
31. Galati F, Rizzo V, Moffa G, et al (2022) Radiologic-pathologic correlation in breast cancer: do MRI biomarkers correlate with pathologic features and molecular subtypes? *Eur Radiol Exp* 6. <https://doi.org/10.1186/s41747-022-00289-7>
32. Matsubayashi R, Matsuo Y, Edakuni G et al (2000) Breast masses with peripheral rim enhancement on dynamic contrast-enhanced MR images: correlation of MR findings with histologic features and expression of growth factors. *Radiology* 217:841–848. <https://doi.org/10.1148/radiology.217.3.r00dc07841>

**Publisher's Note** Springer Nature remains neutral with regard to jurisdictional claims in published maps and institutional affiliations.

Springer Nature or its licensor (e.g. a society or other partner) holds exclusive rights to this article under a publishing agreement with the author(s) or other rightsholder(s); author self-archiving of the accepted manuscript version of this article is solely governed by the terms of such publishing agreement and applicable law.